The Chemical Origins of Plasma Contraction and Thermalization in CO2 Microwave Discharges

Document status and date:
Published: 10/02/2022

DOI:
10.1021/acs.jpclett.1c03731

Document Version:
Publisher's PDF, also known as Version of record

Document license:
Taverne

Please check the document version of this publication:

• A submitted manuscript is the version of the article upon submission and before peer-review. There can be important differences between the submitted version and the official published version of record. People interested in the research are advised to contact the author for the final version of the publication, or visit the DOI to the publisher's website.
• The final author version and the galley proof are versions of the publication after peer review.
• The final published version features the final layout of the paper including the volume, issue and page numbers.

Link to publication

Download date: 28 Apr. 2024

Letter

The Chemical Origins of Plasma Contraction and Thermalization in CO₂ Microwave Discharges

A. W. van de Steeg,[§] L. Vialetto,[§] A. F. Sovelas da Silva, P. Viegas, P. Diomede, M. C. M. van de Sanden, and G. J. van Rooij*

Cite This: *J. Phys. Chem. Lett.* 2022, 13, 1203−1208

Read Online

ACCESS | Metrics & More | Article Recommendations

ABSTRACT: Thermalization of electron and gas temperature in CO₂ microwave plasma is unveiled with the first Thomson scattering measurements. The results contradict the prevalent picture of an increasing electron temperature that causes discharge contraction. It is known that as pressure increases, the radial extension of the plasma reduces from ∼7 mm diameter at 100 mbar to ∼2 mm at 400 mbar. We find that, simultaneously, the initial nonequilibrium between ∼2 eV electron and ∼0.5 eV gas temperature reduces until thermalization occurs at 0.6 eV. 1D fluid modeling, with excellent agreement with measurements, demonstrates that associative ionization of radicals, a mechanism previously proposed for air plasma, causes the thermalization. In effect, heavy particle and heat transport and thermal chemistry govern electron dynamics, a conclusion that provides a basis for ab initio prediction of power concentration in plasma reactors.
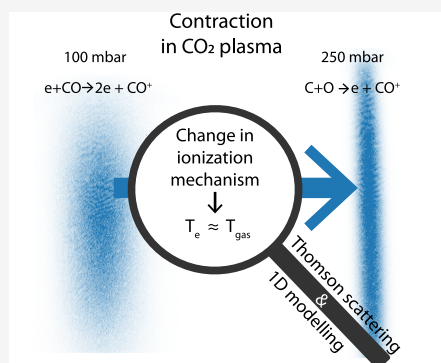
The splitting of CO₂ to CO in (microwave) plasma can be a key technology for CO₂ utilization by providing a carbon-based feedstock for chemicals and fuels.[1−3] This, in turn, can be used for storage of intermittent renewable energy in chemical bonds[4] or integration of, for example, aviation with renewable energy sources.[5] Understanding and predicting the local power input in such plasma systems define which chemical routes are predominant[6−8] and are thus a crucial aspect for reactor engineering. As such, knowledge on the electron properties in the discharge is crucial; the free plasma electrons absorb microwave power and transfer this energy to the heavy particles. A manifestation of the importance of the electron properties, and its influence on dissociation efficiency, is power concentration in the form of plasma contraction.[9−12] Increasing pressure shrinks the plasma in diameter, from ∼7 mm at 80 mbar to ∼2 mm at pressures above 200 mbar, where the various modes of operation have been reported by Wolf et al.[9,13] The energy efficiency changes significantly between these two operating regimes, with reported optimum efficiencies obtained at conditions corresponding to the regime between the two modes.[10,12,14]

The contraction of the discharge is accompanied by an increase in peak gas temperature (T_g): from 3000 to 4000 K at low pressure to more than 6000 K at high pressure.[8−10] Concurrently, the electron number density (n_e) and ionization fraction have been shown to increase by an order of magnitude.[9] On the basis of these measurements, Wolf et al.[13] have argued that the plasma contraction is governed by a thermo-chemical instability.[15] In this theory, a thermal

ionization instability,[16] based on electron impact ionization, links gas temperature, electron temperature (T_e), and n_e in a positive feedback loop, while endothermic reactions impose a limit on the growth of the gas temperature. Nevertheless, uncertainties remain, particularly on the trends in electron temperature and the nature of the instability.

Numerically, Viegas et al.[17] have used the experimental data from Wolf et al.[9] to study the composition of the plasma core by means of a 0D chemical kinetics model. To accommodate the increase in electron number density with contraction, the authors have predicted an increase in ionization frequency and consequently an increase in electron temperature from approximately 1.6 to 2 eV going from low to high pressure. Pietanza et al.[18] have also studied the same system using a 0D plasma chemical kinetics model and calculate electron temperatures to increase with contraction, from 1 to 1.5 eV. The predictions of both models are in accordance with the theory of a thermal ionization instability based on electron impact ionization. Because of the lack of experimental data in the plasma core, neither model has been validated.
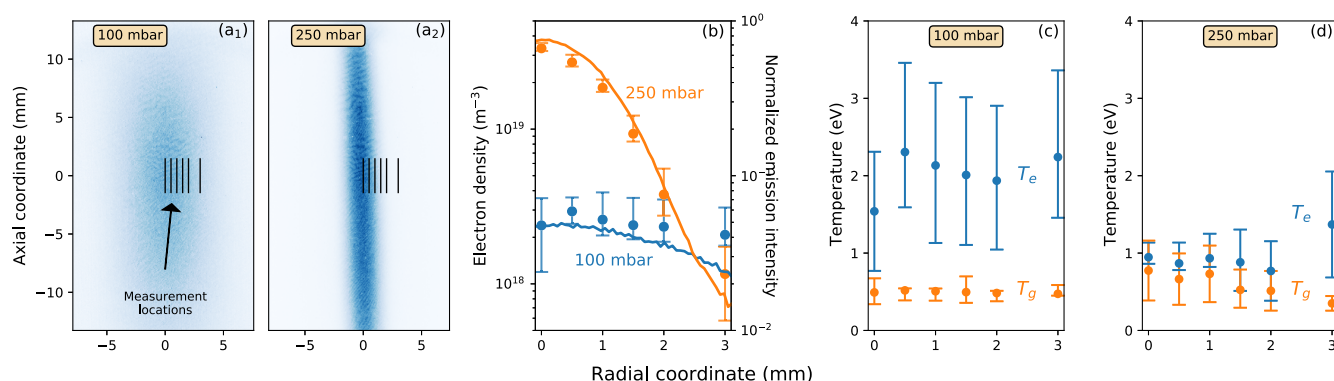
Experimentally, electron temperatures have been estimated by D'Isa et al.[10] by calculating an excitation temperature of
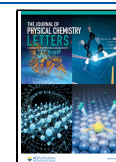
Figure 1. Effect of power concentration for two representative pressures, 100 and 250 mbar, on (a) plasma emission, (b) electron number density (dots) and binned 777 nm oxygen emission (line), (c) electron and gas temperature of 100 mbar, L-mode plasma, and (d) electron and gas temperature of 250 mbar, H-mode plasma. Locations of Thomson−Raman measurements with respect to plasma emission are indicated by black lines in panels a_1 and a_2. Thomson measurements at $r > 3$ mm were not feasible because of the rapidly increasing intensity of CO_2 rotational Raman signature.

atomic species through optical emission spectroscopy and assuming this is a proxy for the electron temperature. This approach shows that excitation temperatures are constant at approximately 0.5 eV, a value equal to the gas temperature in the contracted regime. As noted by the authors, this result contradicts previous modeling efforts and further investigations into electron properties in CO_2 microwave plasma are required.

In this work, we combine Thomson scattering experiments and 1D numerical modeling to assess the contraction mechanisms and to thereby provide a basis for predicting the power concentration. Combined Thomson−Raman scattering yields spatially resolved values of T_e and n_e as well as rotational (assumed equal to translational/gas) temperatures and species concentrations of CO_2, CO, O_2, and O, as shown in our previous work.[8,19] Numerically, a native 1D radial fluid model, elsewhere validated against measurements of neutral species mole fractions, gas temperature, electron number density, and electron temperature, is used to interpret measured trends in electron properties. More details as well as the validation of the model can be found in the work of Vialetto et al.[20]

Figure 1 shows the radially resolved results for the electron temperature and density, the gas temperature, and the 777 nm atomic oxygen emission for two plasma conditions, 100 mbar and 250 mbar, within the first 3 mm of the discharge center. These two conditions are close to the conditions studied in the work of Pietanza et al.[18] and illustrate the effects of power concentration from the (according to the definitions of Wolf et al.[13]) L-mode to the H-mode. Within the large error margins, it can be seen that the 100 mbar L-mode plasma has relatively homogeneous radial profiles of all properties studied with a clear electron-heavy particle nonequilibrium. On the other hand, the 250 mbar H-mode plasma has a peaked and localized emission and electron number density profile, where electron and gas temperature are equal within error margins in the core.

While the large increase in electron number density upon contracting to the H-mode is in accordance with the measurements of Wolf et al.,[9] the decrease in electron temperature contradicts the prevailing theory of a thermal ionization instability[13,15,16] and is not predicted by recently published plasma-chemical models[17,18] or experiments.[10] These aspects are highlighted in Figure 2, where experimental and numerical results of the present work and recent studies

are shown as a function of pressure for the central plasma position ($r = 0$ mm).
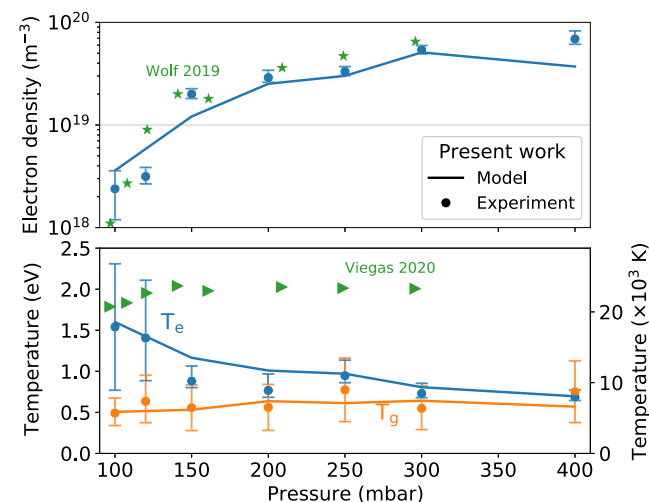
Figure 2. Experimental and numerical results for (top) the electron number density and (bottom) the electron and gas temperatures in the radial center of the plasma as a function of pressure. In red, previous measurements of n_e reported by Wolf et al.[9] and numerical results of T_e of Viegas et al.[17] for an identical plasma system (with 1400 W input power).

Experimental results of the present study show that the electron number density in the plasma core (top) increases by an order of magnitude. The measured values show excellent quantitative agreement with the line-integrated n_e measurements of Wolf et al.[9] The electron temperature (bottom) decreases by a factor 2 from low to high pressure, and gas temperature increases slightly, until both temperatures equilibrate within the error margin of the experiment at approximately 200 mbar. This trend contradicts the results of the modeling study of Viegas et al.,[17] who predict a slight increase in core electron temperature.

A 1D radial model has been developed by the present authors to disclose the mechanism behind the observed plasma thermalization. Results of the model, included in Figure 2 (solid line), show good overlap with experimental results; both the order of magnitude increase in n_e as well as the decrease in
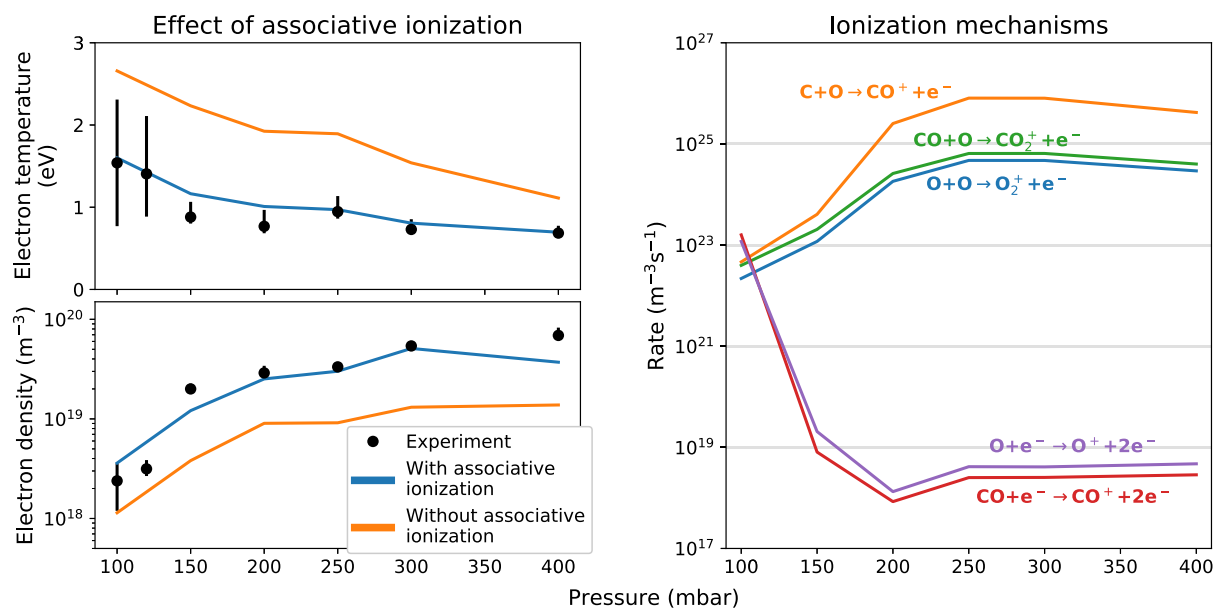
Figure 3. Left: Effect of associative ionization on electron temperature (top) and electron number density (bottom), illustrated by comparing experimental and numerical results of the base model and the model excluding all associative ionization reactions. Right: Rates of the main ionization reactions as calculated by the model, which thus depend on the calculated gas and electron temperature and species densities.

T_e and subsequent thermalization with T_g are predicted accurately. The model takes the majority of the chemical reactions from the work by Viegas et al.[17] The key changes to the chemistry affect the charged particle sources. Two types of ionization mechanisms are included: (i) direct electron impact ionization of atoms/molecules in the ground electronic state and (ii) associative ionization mediated by the high gas temperature and association of radicals.

The second mechanism, associative ionization, is particularly important. This ionization source is often overlooked in plasma-chemical models but plays a crucial role in the studied plasma. Associative ionization reactions of C, O, and CO species are included in this work and that of Viegas et al.[17] The latter, however, state that the process is not of importance in the discharge. The present model uses a different rate constant for the C + O associative ionization reaction:[21]

$$k_{C+O \rightarrow CO^+ + e} = 8.78 \times 10^{-12} (\text{cm}^3\,\text{s}^{-1}) \exp\left(-\frac{33100(\text{K})}{T_g}\right)$$
(1)

As noted by Viegas et al.,[17] at 6000 K this rate constant is 3 orders of magnitude higher than the rate constant used in that work, mainly because of a very different activation energy. In the recent work by Sun et al.,[22] an atmospheric pressure CO_2 microwave plasma is investigated; therein, the authors consider a similar rate constant as eq 1 and claim that this reaction is the dominant source of charged particles. In the work by Vialetto et al.[20] the choice of the rate constant for associative ionization is described in more detail; moreover, it presents a sensitivity study on the choice of the rate constant.

The importance of the associative ionization mechanism in the model to obtain a good agreement with experiments is highlighted on the left-hand side of Figure 3. Here, the electron temperature and electron number density of the model with and without associative ionization are compared with measurements. Without associative ionization, both electron temperature and density deviate significantly from measured values. It

is interesting to note that even without associative ionization, the model predicts the trends in n_e and T_e (but not the thermalization). This is a result of the different numerical approach (see Numerical Methods and Vialetto et al.[20]), particularly the addition of an electron mean energy equation and heat equation in the calculation of the electric field.

The large differences in absolute n_e and T_e values can be understood by comparing the rates for different ionization reactions, shown on the right-hand side of Figure 3, where from low to high pressure a shift in the dominant ionization mechanism can be observed. At low pressure, the electron impact ionization dominates, whereas at high pressure, the associative ionization of C + O is the principal source of charged species. The numerical study of Benilov and Naidis[23] predicts a similar change in ionization mechanism with increasing current in a low-current arc discharge in air at atmospheric pressure.

In previous studies, electron-impact ionization and electron−ion dissociative recombination are assumed to be the main electron production and loss mechanisms. As such, the charge balance is approximated as[9,17,18]

$$n_e n_g k_i(T_e) = n_e n_{MI} k_{rec}(T_e) \rightarrow \frac{n_{MI}}{n_g} = \frac{k_i(T_e)}{k_{rec}(T_e)}$$
(2)

Here, n_g is the gas number density; k_i is an effective electron impact ionization rate constant, depending on the composition and electron temperature; k_{rec} is an effective recombination rate constant, weakly dependent on the electron temperature; and n_{MI} is the molecular ion number density. Considering the presented results, the charge balance in contracted (H-mode) conditions can be described as

$$[C][O]k_{C+O \rightarrow CO^+ + e}(T_g) = n_e n_{MI} k_{rec}(T_e)$$
(3)

The predominance of associative ionization as charge source term directly links gas temperature and composition with electron properties in the plasma core. In effect, the electron and thermal properties in contracted CO_2 microwave plasma
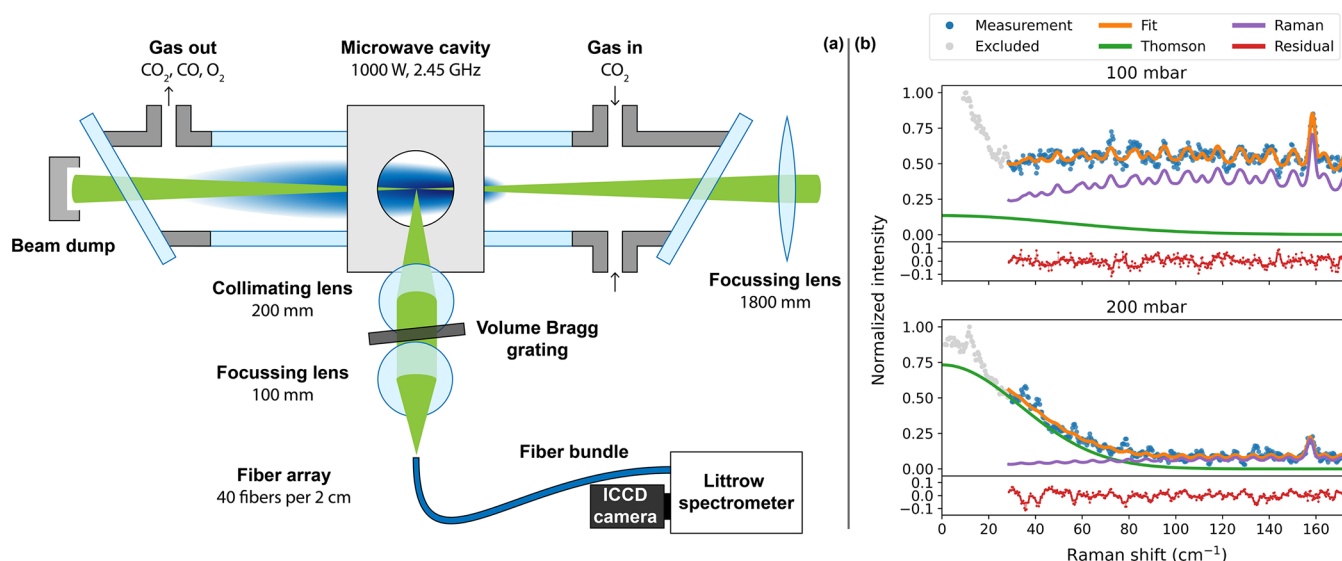
Figure 4. Left: Schematic of the combined microwave plasma–laser scattering setup. Right: Two representative measured spectra of combined Thomson-Raman scattering. Top: low n_e, high CO_2 fraction (100 mbar). Bottom: high n_e, low CO_2 fraction (200 mbar).

become interdependent: the gas temperature is defined by transport processes and the power density deposited by electrons and, in turn, provides the composition and associative ionization rate coefficient which determine charge balance and electron properties. These described processes lead to a circular dependency that explains the radial contraction: an increasing core temperature increases the rate of associative ionization. To balance eq 3, either the electron number density increases (or the electron temperature decreases), where a rise in electron number density leads to an increase in power density and thus to a further rise in gas temperature.

This finding changes the understanding of the contraction phenomenon from L-mode to H-mode in CO_2 microwave discharges; before the thermal ionization instability was presumed to play a crucial role, while these results show that a self-intensifying rise in gas temperature and electron number density, mediated by associative ionization, provides the instability. As to why contraction occurs with increasing pressure, Wolf et al.[14] have shown turbulent radial transport decreases by more than an order of magnitude in the pressure range investigated. This leads to a natural increase in gas temperature with pressure, which instigates the associative ionization mediated instability.

In conclusion, the combined experimental and numerical effort has shown the importance of thermal chemistry, and particularly associative ionization of atoms, in the equilibration of electron and gas temperature in CO_2 microwave plasma. As such, trends of T_e and T_g as a function of pressure become remarkably similar to textbook examples of thermalizing discharges (e.g., argon arcs)[24] and contradict recent modeling works as well as the generally assumed electron-heavy particle nonequilibrium nature of the discharge. By showing the importance of heavy species properties on electron kinetics, and by extension the local power absorption, this work provides a new description of the contraction phenomenon and lays a foundation for predicting power concentration in the engineering of plasma reactors.

■ EXPERIMENTAL METHODS

Details of the microwave and vacuum setup have been reported before.[12] Briefly, laser scattering is coupled to a microwave plasma setup as schematically illustrated in Figure 4a. A 2.45 GHz magnetron of 1 kW input power provides microwaves to the plasma, generated in a quartz tube of 27 mm inner diameter. Tangentially injected CO_2 (99.995% purity) gas with a mass flow rate of 10 l/min (at standard pressure and temperature) creates a swirl flow in the tube to protect the walls from overheating. A frequency-doubled Nd:YAG laser (30 Hz, 400 mJ per 10 ns pulse, 532 nm) is focused into the reactor. Scattered light of the focal point of the laser is collimated by a 200 mm lens. A volume Bragg grating strongly attenuates the 532 nm component of the collimated light, which is subsequently focused by a 100 mm lens into a linear fiber array. This relays the scattered light into a 1 m focal distance and 50 μm entrance slit custom-built Littrow spectrometer equipped with an 1800 l/mm grating and a resulting dispersion of 0.012 nm/pixel. The spectrally resolved image is captured by an intensified camera.

Previously, the application of Thomson scattering in CO_2 plasma has been challenging because of the low ionization degree[9] and high rotational Raman and Rayleigh signal strengths of CO_2,[25] obfuscating the Thomson signature. The successful implementation of the diagnostic in this study is made possible by the combination of a volume Bragg grating (serving as narrowband notch filter[26]), high gas temperature (reducing and distributing the rotational Raman intensity over a wider spectral range), and high dissociation degree (reducing effective rotational Raman cross section and thus intensity[19]). Similar to Vincent et al.,[27] we use a linear fiber array in combination with the Bragg grating: 8 fibers are simultaneously imaged unto the camera, increasing total signal strength.

Possible perturbations of the diagnostics (e.g., photoionization), have been investigated by an attenuation of the laser power to half its original value for several key measurements. This resulted in identical values of electron properties, proving the nonintrusiveness of the diagnostics.

Figure 4b illustrates the complicating presence of the rotational Raman spectrum for achieving sensitivity toward

the Thomson signature on the basis of two representing conditions: a 100 mbar plasma with low n_e (top) and a 200 mbar plasma with high n_e (bottom). Illustrated in these spectra are two effects on the sensitivity to Thomson signal: (i) the stray light feature at low Raman shifts, a result of the integration of the Bragg grating with the collection optics, decreasing the attenuation of stray light, and (ii) the increase in the C_2 optical emission[10] (and laser-induced fluorescence[19]) with increasing pressure. Nevertheless, the wide spectral profile of the Thomson scattering is fitted accurately in the presence of both C_2 emission and stray light. However, the fitting of the narrower Raman signature gets perturbed by the C_2 emission, introducing a large uncertainty in the determination of gas temperature at high pressure, with error margins up to ∼50%. At low pressure, C_2 emission is absent, but the Raman signal of CO_2 is much stronger than the Thomson signal, and both electron temperature and density have large error margins also up to ∼50%. Precise values of uncertainty were determined with the method described in our previous work.[8]

Spectra are fitted to a synthetic spectrum comprising the rotational Raman contributions of the molecular species, CO_2, CO, O_2, the atomic Raman of O, and the Thomson signature. The treatment of Raman data and atomic oxygen quantification was the topic of our previous work.[19] The (incoherent) Thomson signal is analyzed following the description of Carbone et al.[28]

NUMERICAL METHODS

The model[20] solves a system of fluid equations for neutral and charged species mass fractions and for the gas temperature.[29] Electron rate and transport coefficients and electron power losses are calculated with a Monte Carlo Flux solver[30,31] that has been coupled to the fluid code. The model computes species mole fractions and electron and gas temperatures for a given radial profile of absorbed microwave power density. The locally dissipated microwave power density used as input for the model is assumed to scale with the 777 nm atomic oxygen emission as in Wolf et al.[13,14]

While the measurements show direct evidence of a C_2 presence (in the form of Swan emission and fluorescence), this species is not considered in the model. In fact, Viegas et al.[17] argue that the species, while strongly emitting, is irrelevant in the description of the main heavy species. Its inclusion would influence the rate of C + O associative ionization, but it is expected that this effect is small.

The changes with respect to the previous model of Viegas et al.[17] (whose results are shown in Figure 2) can be summarized as (i) a 1D radial approach, as opposed to a 0D approach applied to the plasma core only; (ii) an adapted chemistry set, with the most notable change to the rate of C + O associative ionization; (iii) the calculation of radial profiles of gas temperature and mean electron energy through energy balance equations; and (iv) the different method of calculating the electric field (and thus T_e). In addition to the particle balance equation used in Viegas et al.,[17] a mean energy equation and a heat equation are implemented.

AUTHOR INFORMATION

Corresponding Author

G. J. van Rooij − DIFFER, 5612AJ Eindhoven, The Netherlands; Faculty of Science and Engineering, Maastricht University, 6229 GS Maastricht, The Netherlands; Email: g.vanrooij@maastrichtuniversity.nl

Authors

A. W. van de Steeg − DIFFER, 5612AJ Eindhoven, The Netherlands; orcid.org/0000-0002-2976-7905

L. Vialetto − DIFFER, 5612AJ Eindhoven, The Netherlands

A. F. Sovelas da Silva − DIFFER, 5612AJ Eindhoven, The Netherlands

P. Viegas − Department of Physical Electronics, Faculty of Science, Masaryk University, 611 37 Brno, Czech Republic; DIFFER, 5612AJ Eindhoven, The Netherlands; orcid.org/0000-0002-3820-3300

P. Diomede − Faculty of Science and Engineering, Maastricht University, 6229 GS Maastricht, The Netherlands; orcid.org/0000-0002-4523-3049

M. C. M. van de Sanden − DIFFER, 5612AJ Eindhoven, The Netherlands; orcid.org/0000-0002-4119-9971

Complete contact information is available at:
https://pubs.acs.org/10.1021/acs.jpclett.1c03731

Author Contributions

Notes

The authors declare no competing financial interest.

REFERENCES

(1) Hepburn, C.; Adlen, E.; Beddington, J.; Carter, E. A.; Fuss, S.; Mac Dowell, N.; Minx, J. C.; Smith, P.; Williams, C. K. The Technological and Economic Prospects for CO_2 Utilization and Removal. Nature 2019, 575 (7781), 87−97.

(2) Snoeckx, R.; Bogaerts, A. Plasma Technology-a Novel Solution for CO_2 Conversion? Chem. Soc. Rev. 2017, 46 (19), 5805−5863.

(3) Grim, R. G.; Huang, Z.; Guarnieri, M. T.; Ferrell, J. R.; Tao, L.; Schaidle, J. A. Transforming the Carbon Economy: Challenges and Opportunities in the Convergence of Low-Cost Electricity and Reductive CO_2 Utilization. Energy Environ. Sci. 2020, 13 (2), 472−494.

(4) Bogaerts, A.; Neyts, E. C. Plasma Technology: An Emerging Technology for Energy Storage. ACS Energy Lett. 2018, 3 (4), 1013−1027.

(5) Becattini, V.; Gabrielli, P.; Mazzotti, M. Role of Carbon Capture, Storage, and Utilization to Enable a Net-Zero-CO_2-Emissions Aviation Sector. Ind. Eng. Chem. Res. 2021, 60 (18), 6848−6862.

(6) Vermeiren, V.; Bogaerts, A. Plasma-Based CO_2 Conversion: To Quench or Not to Quench? J. Phys. Chem. C 2020, 124 (34), 18401−18415.

(7) Trenchev, G.; Bogaerts, A. Dual-Vortex Plasmatron: A Novel Plasma Source for CO_2 Conversion. J. CO2 Util. 2020, 39, 101152.

(8) Van De Steeg, A.; Viegas, P.; Silva, A.; Butterworth, T.; Van Bavel, A.; Smits, J.; Diomede, P.; van de Sanden, M.; Van Rooij, G. Redefining the Microwave Plasma-Mediated CO_2 Reduction Efficiency Limit: The Role of O − CO_2 Association. ACS Energy Lett. 2021, 6, 2876−2881.

(9) Wolf, A. J.; Righart, T. W. H.; Peeters, F.; Groen, P. W. C.; Van de Sanden, M. C. M.; Bongers, W. Characterization of the CO_2 Microwave Plasma Based on the Phenomenon of Skin Depth-Limited Contraction. *Plasma Sources Sci. Technol.* **2019**, *28*, 115022.

(10) D'Isa, F. A.; Carbone, E. A. D.; Hecimovic, A.; Fantz, U. Performance Analysis of a 2.45 GHz Microwave Plasma Torch for CO_2 Decomposition in Gas Swirl Configuration. *Plasma Sources Sci. Technol.* **2020**, *29*, 105009.

(11) Fridman, A. *Plasma Chemistry*, 1st ed.; Cambridge University Press, 2008. DOI: 10.1192/bjp.111.479.1009-a.

(12) den Harder, N.; Van den Bekerom, D. C. M.; Al, R. S.; Graswinckel, M. F.; Palomares, J. M.; Peeters, F. J. J.; Ponduri, S.; Minea, T.; Bongers, W. A.; van de Sanden, M. C. M.; van Rooij, G. J. Homogeneous CO_2 Conversion by Microwave Plasma: Wave Propagation and Diagnostics. *Plasma Process. Polym.* **2017**, *14* (6), 1600120.

(13) Wolf, A. J.; Righart, T. W. H.; Peeters, F. J. J.; Bongers, W. A.; Van De Sanden, M. C. M. Implications of Thermo-Chemical Instability on the Contracted Modes in CO_2 Microwave Plasmas. *Plasma Sources Sci. Technol.* **2020**, *29* (2), 025005.

(14) Wolf, A. J. J.; Peeters, F. J. J.; Groen, P. W. C.; Bongers, W. A.; Van De Sanden, M. C. M. CO_2 Conversion in Nonuniform Discharges: Disentangling Dissociation and Recombination Mechanisms. *J. Phys. Chem. C* **2020**, *124* (31), 16806−16819.

(15) Zhong, H.; Shneider, M. N.; Mokrov, M. S.; Ju, Y. Thermal-Chemical Instability of Weakly Ionized Plasma in a Reactive Flow. *J. Phys. D. Appl. Phys.* **2019**, *52* (48), 484001.

(16) Fridman, A. A. .; Kennedy, L. A. *Plasma Physics and Engineering*; Taylor & Francis: New York, 2004.

(17) Viegas, P.; Vialetto, L.; Wolf, A. J.; Peeters, F.; Groen, P. W. C.; Righart, T. W. H.; Bongers, W.; Van de Sanden, M. C. M.; Diomede, P. Insight into Contraction Dynamics of Microwave Plasmas for CO_2 Conversion from Plasma Chemistry Modelling. *Plasma Sources Sci. Technol.* **2020**, *29*, 105014.

(18) Pietanza, L. D.; Colonna, G.; Capitelli, M. Kinetics versus Thermodynamics on CO_2 Dissociation in High Temperature Microwave Discharges. *Plasma Sources Sci. Technol.* **2020**, *29* (3), 035022.

(19) Van de Steeg, A. W.; Vialetto, L.; Silva, A. F.; Peeters, F. J. J.; Van den Bekerom, D. C. M.; Gatti, N.; Diomede, P.; Van de Sanden, M. C. M.; Van Rooij, G. J. Revisiting Spontaneous Raman Scattering for Direct Oxygen Atom Quantification. *Opt. Lett.* **2021**, *46* (9), 2172−2175.

(20) Vialetto, L.; van de Steeg, A. W.; Viegas, P.; Longo, S.; van Rooij, G. J.; van de Sanden, M. C. M.; Van Dijk, J.; Diomede, P. Investigation of CO_2 Microwave Discharges through Comparisons between Simulations and Experiments: Role of Charged Particle Kinetics and Gas Heating on Plasma Contraction. Submitted to *Plasma Sources Sci. Technol.*

(21) Park, C.; Howe, J. T.; Jaffe, R. L.; Candler, G. V. Review of Chemical-Kinetic Problems of Future NASA Missions, II: Mars Entries. *J. Thermophys. Heat Transfer* **1994**, *8* (1), 9−23.

(22) Sun, H.; Lee, J.; Do, H.; Im, S. K.; Soo Bak, M. Experimental and Numerical Studies on Carbon Dioxide Decomposition in Atmospheric Electrodeless Microwave Plasmas. *J. Appl. Phys.* **2017**, *122*, 033303.

(23) Benilov, M. S.; Naidis, G. V. Modelling of Low-Current Discharges in Atmospheric-Pressure Air Taking Account of Non-Equilibrium Effects. *J. Phys. D. Appl. Phys.* **2003**, *36* (15), 1834−1841.

(24) Roth, J. R. *Industrial Plasma Engineering*; Institute of Physics Publishing: London, 1995.

(25) Penney, C. M.; St. Peters, R. L.; Lapp, M. Absolute Rotational Raman Cross Sections for N_2, O_2 and CO_2. *J. Opt. Soc. Am.* **1974**, *64* (5), 712−716.

(26) Klarenaar, B. L. M.; Brehmer, F.; Welzel, S.; Van Der Meiden, H. J.; Van De Sanden, M. C. M.; Engeln, R. Note: Rotational Raman Scattering on CO_2 Plasma Using a Volume Bragg Grating as a Notch Filter. *Rev. Sci. Instrum.* **2015**, *86* (4), 046106.

(27) Vincent, B.; Tsikata, S.; Mazouffre, S.; Minea, T.; Fils, J. A Compact New Incoherent Thomson Scattering Diagnostic for Low-Temperature Plasma Studies. *Plasma Sources Sci. Technol.* **2018**, *27* (5), 055002.

(28) Carbone, E.; Nijdam, S. Thomson Scattering on Non-Equilibrium Low Density Plasmas: Principles, Practice and Challenges. *Plasma Phys. Control. Fusion* **2015**, *57* (1), 014026.

(29) Hassouni, K.; Leroy, O.; Farhat, S.; Gicquel, A. Modeling of H_2 and H_2/CH_4 Moderate-Pressure Microwave Plasma Used for Diamond Deposition. *Plasma Chem. Plasma Process.* **1998**, *18* (3), 325−362.

(30) Vialetto, L.; Viegas, P.; Longo, S.; Diomede, P. Benchmarking of Monte Carlo Flux Simulations of Electrons in CO_2. *Plasma Sources Sci. Technol.* **2020**, *29* (11), 115006.

(31) Vialetto, L.; Longo, S.; Diomede, P. Benchmark Calculations for Electron Velocity Distribution Function Obtained with Monte Carlo Flux Simulations. *Plasma Sources Sci. Technol.* **2019**, *28* (11), 115015.